

Bose-Einstein Correlations of π^0 Pairs from Hadronic Z^0 Decays

The OPAL Collaboration

Abstract

We observe Bose-Einstein correlations in π^0 pairs produced in Z^0 hadronic decays using the data sample collected by the OPAL detector at LEP 1 from 1991 to 1995. Using a static Gaussian picture for the pion emitter source, we obtain the chaoticity parameter $\lambda = 0.55 \pm 0.10 \pm 0.10$ and the source radius $R = (0.59 \pm 0.08 \pm 0.05)$ fm. According to the JETSET and HERWIG Monte Carlo models, the Bose-Einstein correlations in our data sample largely connect π^0 s originating from the decays of different hadrons. Prompt pions formed at string break-ups or cluster decays only form a small fraction of the sample.

(Submitted to Physics Letters B)

The OPAL Collaboration

G. Abbiendi², C. Ainsley⁵, P.F. Åkesson³, G. Alexander²², J. Allison¹⁶, P. Amaral⁹, G. Anagnostou¹, K.J. Anderson⁹, S. Arcelli², S. Asai²³, D. Axen²⁷, G. Azuelos^{18,a}, I. Bailey²⁶, E. Barberio^{8,p}, R.J. Barlow¹⁶, R.J. Batley⁵, P. Bechtel²⁵, T. Behnke²⁵, K.W. Bell²⁰, P.J. Bell¹, G. Bella²², A. Bellerive⁶, G. Benelli⁴, S. Bethke³², O. Biebel³¹, I.J. Bloodworth¹, O. Boeriu¹⁰, P. Bock¹¹, D. Bonacorsi², M. Boutemur³¹, S. Braibant⁸, L. Brigliadori², R.M. Brown²⁰, K. Buesser²⁵, H.J. Burckhart⁸, S. Campana⁴, R.K. Carnegie⁶, B. Caron²⁸, A.A. Carter¹³, J.R. Carter⁵, C.Y. Chang¹⁷, D.G. Charlton^{1,b}, A. Csilling^{8,g}, M. Cuffiani², S. Dado²¹, A. De Roeck⁸, E.A. De Wolf^{8,s}, K. Desch²⁵, B. Dienes³⁰, M. Donkers⁶, J. Dubbert³¹, E. Duchovni²⁴, G. Duckeck³¹, I.P. Duerdoth¹⁶, E. Elfgrén¹⁸, E. Etzion²², F. Fabbri², L. Feld¹⁰, P. Ferrari⁸, F. Fiedler³¹, I. Fleck¹⁰, M. Ford⁵, A. Frey⁸, A. Fürtjes⁸, P. Gagnon¹², J.W. Gary⁴, G. Gaycken²⁵, C. Geich-Gimbel³, G. Giacomelli², P. Giacomelli², M. Giunta⁴, J. Goldberg²¹, E. Gross²⁴, J. Grunhaus²², M. Gruwe⁸, P.O. Günther³, A. Gupta⁹, C. Hajdu²⁹, M. Hamann²⁵, G.G. Hanson⁴, K. Harder²⁵, A. Harel²¹, M. Harin-Dirac⁴, M. Hauschild⁸, C.M. Hawkes¹, R. Hawkings⁸, R.J. Hemingway⁶, C. Hensel²⁵, G. Herten¹⁰, R.D. Heuer²⁵, J.C. Hill⁵, K. Hoffman⁹, R.J. Homer¹, D. Horváth^{29,c}, P. Igo-Kemenes¹¹, K. Ishii²³, H. Jeremie¹⁸, P. Jovanovic¹, T.R. Junk⁶, N. Kanaya²⁶, J. Kanzaki²³, G. Karapetian¹⁸, D. Karlen⁶, K. Kawagoe²³, T. Kawamoto²³, R.K. Keeler²⁶, R.G. Kellogg¹⁷, B.W. Kennedy²⁰, D.H. Kim¹⁹, K. Klein^{11,t}, A. Klier²⁴, S. Kluth³², T. Kobayashi²³, M. Kobel³, S. Komamiya²³, L. Kormos²⁶, T. Krämer²⁵, T. Kress⁴, P. Krieger^{6,l}, J. von Krogh¹¹, D. Krop¹², K. Kruger⁸, T. Kuhl²⁵, M. Kupper²⁴, G.D. Lafferty¹⁶, H. Landsman²¹, D. Lanske¹⁴, J.G. Layter⁴, A. Leins³¹, D. Lellouch²⁴, J. Letts^o, L. Levinson²⁴, J. Lillich¹⁰, S.L. Lloyd¹³, F.K. Loebinger¹⁶, J. Lu²⁷, J. Ludwig¹⁰, A. Macpherson^{28,i}, W. Mader³, S. Marcellini², A.J. Martin¹³, G. Masetti², T. Mashimo²³, P. Mättig^m, W.J. McDonald²⁸, J. McKenna²⁷, T.J. McMahon¹, R.A. McPherson²⁶, F. Meijers⁸, W. Menges²⁵, F.S. Merritt⁹, H. Mes^{6,a}, A. Michelini², S. Mihara²³, G. Mikenberg²⁴, D.J. Miller¹⁵, S. Moed²¹, W. Mohr¹⁰, T. Mori²³, A. Mutter¹⁰, K. Nagai¹³, I. Nakamura²³, H.A. Neal³³, R. Nisius³², S.W. O’Neale¹, A. Oh⁸, A. Okpara¹¹, M.J. Oreglia⁹, S. Orito²³, C. Pahl³², G. Pásztor^{4,g}, J.R. Pater¹⁶, G.N. Patrick²⁰, J.E. Pilcher⁹, J. Pinfold²⁸, D.E. Plane⁸, B. Poli², J. Polok⁸, O. Pooth¹⁴, M. Przybycień^{8,n}, A. Quadt³, K. Rabbertz^{8,r}, C. Rembser⁸, P. Renkel²⁴, H. Rick⁴, J.M. Roney²⁶, S. Rosati³, Y. Rozen²¹, K. Runge¹⁰, K. Sachs⁶, T. Saeki²³, E.K.G. Sarkisyan^{8,j}, A.D. Schaile³¹, O. Schaile³¹, P. Scharff-Hansen⁸, J. Schieck³², T. Schörner-Sadenius⁸, M. Schröder⁸, M. Schumacher³, C. Schwick⁸, W.G. Scott²⁰, R. Seuster^{14,f}, T.G. Shears^{8,h}, B.C. Shen⁴, P. Sherwood¹⁵, G. Siroli², A. Skuja¹⁷, A.M. Smith⁸, R. Sobie²⁶, S. Söldner-Rembold^{16,d}, F. Spano⁹, A. Stahl³, K. Stephens¹⁶, D. Strom¹⁹, R. Ströhmer³¹, S. Tarem²¹, M. Tasevsky⁸, R.J. Taylor¹⁵, R. Teuscher⁹, M.A. Thomson⁵, E. Torrence¹⁹, D. Toya²³, P. Tran⁴, A. Tricoli², I. Trigger⁸, Z. Trócsányi^{30,e}, E. Tsur²², M.F. Turner-Watson¹, I. Ueda²³, B. Ujvári^{30,e}, C.F. Vollmer³¹, P. Vannerem¹⁰, R. Vértesi³⁰, M. Verzocchi¹⁷, H. Voss^{8,q}, J. Vossebeld^{8,h}, D. Waller⁶, C.P. Ward⁵, D.R. Ward⁵, P.M. Watkins¹, A.T. Watson¹, N.K. Watson¹, P.S. Wells⁸, T. Wengler⁸, N. Wormes³, D. Wetterling¹¹, G.W. Wilson^{16,k}, J.A. Wilson¹, G. Wolf²⁴, T.R. Wyatt¹⁶, S. Yamashita²³, D. Zer-Zion⁴, L. Zivkovic²⁴

¹School of Physics and Astronomy, University of Birmingham, Birmingham B15 2TT, UK

²Dipartimento di Fisica dell’ Università di Bologna and INFN, I-40126 Bologna, Italy

- ³Physikalisches Institut, Universität Bonn, D-53115 Bonn, Germany
- ⁴Department of Physics, University of California, Riverside CA 92521, USA
- ⁵Cavendish Laboratory, Cambridge CB3 0HE, UK
- ⁶Ottawa-Carleton Institute for Physics, Department of Physics, Carleton University, Ottawa, Ontario K1S 5B6, Canada
- ⁸CERN, European Organisation for Nuclear Research, CH-1211 Geneva 23, Switzerland
- ⁹Enrico Fermi Institute and Department of Physics, University of Chicago, Chicago IL 60637, USA
- ¹⁰Fakultät für Physik, Albert-Ludwigs-Universität Freiburg, D-79104 Freiburg, Germany
- ¹¹Physikalisches Institut, Universität Heidelberg, D-69120 Heidelberg, Germany
- ¹²Indiana University, Department of Physics, Bloomington IN 47405, USA
- ¹³Queen Mary and Westfield College, University of London, London E1 4NS, UK
- ¹⁴Technische Hochschule Aachen, III Physikalisches Institut, Sommerfeldstrasse 26-28, D-52056 Aachen, Germany
- ¹⁵University College London, London WC1E 6BT, UK
- ¹⁶Department of Physics, Schuster Laboratory, The University, Manchester M13 9PL, UK
- ¹⁷Department of Physics, University of Maryland, College Park, MD 20742, USA
- ¹⁸Laboratoire de Physique Nucléaire, Université de Montréal, Montréal, Québec H3C 3J7, Canada
- ¹⁹University of Oregon, Department of Physics, Eugene OR 97403, USA
- ²⁰CLRC Rutherford Appleton Laboratory, Chilton, Didcot, Oxfordshire OX11 0QX, UK
- ²¹Department of Physics, Technion-Israel Institute of Technology, Haifa 32000, Israel
- ²²Department of Physics and Astronomy, Tel Aviv University, Tel Aviv 69978, Israel
- ²³International Centre for Elementary Particle Physics and Department of Physics, University of Tokyo, Tokyo 113-0033, and Kobe University, Kobe 657-8501, Japan
- ²⁴Particle Physics Department, Weizmann Institute of Science, Rehovot 76100, Israel
- ²⁵Universität Hamburg/DESY, Institut für Experimentalphysik, Notkestrasse 85, D-22607 Hamburg, Germany
- ²⁶University of Victoria, Department of Physics, P O Box 3055, Victoria BC V8W 3P6, Canada
- ²⁷University of British Columbia, Department of Physics, Vancouver BC V6T 1Z1, Canada
- ²⁸University of Alberta, Department of Physics, Edmonton AB T6G 2J1, Canada
- ²⁹Research Institute for Particle and Nuclear Physics, H-1525 Budapest, P O Box 49, Hungary
- ³⁰Institute of Nuclear Research, H-4001 Debrecen, P O Box 51, Hungary
- ³¹Ludwig-Maximilians-Universität München, Sektion Physik, Am Coulombwall 1, D-85748 Garching, Germany
- ³²Max-Planck-Institute für Physik, Föhringer Ring 6, D-80805 München, Germany
- ³³Yale University, Department of Physics, New Haven, CT 06520, USA

^a and at TRIUMF, Vancouver, Canada V6T 2A3

^b and Royal Society University Research Fellow

^c and Institute of Nuclear Research, Debrecen, Hungary

^d and Heisenberg Fellow

^e and Department of Experimental Physics, Lajos Kossuth University, Debrecen, Hungary

^f and MPI München

^g and Research Institute for Particle and Nuclear Physics, Budapest, Hungary
^h now at University of Liverpool, Dept of Physics, Liverpool L69 3BX, U.K.
ⁱ and CERN, EP Div, 1211 Geneva 23
^j now at University of Nijmegen, HEFIN, NL-6525 ED Nijmegen, The Netherlands, on NWO/NATO Fellowship B 64-29
^k now at University of Kansas, Dept of Physics and Astronomy, Lawrence, KS 66045, U.S.A.
^l now at University of Toronto, Dept of Physics, Toronto, Canada
^m current address Bergische Universität, Wuppertal, Germany
ⁿ and University of Mining and Metallurgy, Cracow, Poland
^o now at University of California, San Diego, U.S.A.
^p now at Physics Dept Southern Methodist University, Dallas, TX 75275, U.S.A.
^q now at IPHE Université de Lausanne, CH-1015 Lausanne, Switzerland
^r now at IEKP Universität Karlsruhe, Germany
^s now at Universitaire Instelling Antwerpen, Physics Department, B-2610 Antwerpen, Belgium
^t now at RWTH Aachen, Germany

1 Introduction

The Bose-Einstein correlations (BEC) effect has a quantum-mechanical origin. It arises from the requirement to symmetrise the wave function of a system of two or more identical bosons. It was introduced into particle reactions leading to multi-hadron final states as the GGLP effect [1] in the study of the $\pi^+\pi^+$ and $\pi^-\pi^-$ systems. The distributions of the opening angle between the momenta in pairs of like-sign pions were shifted towards smaller values compared to the corresponding distributions for unlike-sign pairs. A related effect was exploited earlier in astronomy [2] to measure the radii of stars.

In high energy physics, for example e^+e^- collisions at LEP, a quantitative understanding of the BEC effect allows tests of the parton fragmentation and hadronisation models. This would in turn help in achieving a more precise measurement of the W boson mass and better knowledge of several Standard Model (SM) observables [3]. The fragmentation models presently used are those of strings and clusters implemented, respectively, in the JETSET [4] and HERWIG [5] Monte Carlo generators.

Numerous studies of BEC in pairs of identical bosons already exist, see for example [6]. Due to the experimental difficulties in photon and π^0 reconstruction, only very few studies [7] exist for BEC in π^0 pairs, even though they offer the advantage of being free of final state Coulomb corrections.

The string model predicts a larger BEC strength or chaoticity and a smaller effective radius of the emitting source for π^0 pairs compared to π^\pm pairs while the cluster fragmentation model predicts the same source strength and size [8, 9]. However, neither model of primary hadron production has a mechanism to allow BEC between π^0 s produced in different

strong decays. The string model prediction is a consequence of electric charge conservation in the local area where the string breaks up. Similar expectations can be derived if the probabilities in the string break-up mechanism are interpreted as the squares of quantum mechanical amplitudes [8, 10]. A small difference between π^\pm pairs and π^0 pairs is also expected from a pure quantum statistical approach to Bose-Einstein symmetry [11]. In addition, based on isospin invariance, suggestions exist on how to relate BEC in the pion-pair systems i.e. $\pi^0\pi^0$, $\pi^\pm\pi^\pm$, and $\pi^+\pi^-$ and how to extend it to $\pi^\pm\pi^0$. [12]. The L3 collaboration has recently reported [7] that the radius of the neutral-pion source may be smaller than that of charged pions, $R_{\pi^\pm\pi^\pm} - R_{\pi^0\pi^0} = (0.150 \pm 0.075(\text{stat.}) \pm 0.068(\text{syst.}))$ fm, in qualitative agreement with the string fragmentation prediction.

This paper presents a study of BEC in π^0 pairs using the full hadronic event sample collected at centre-of-mass energies at and near the Z^0 peak by the OPAL detector at LEP from 1991 to 1995. This corresponds to about four million hadronic Z^0 decays. A highly pure sample of π^0 mesons is reconstructed using the lead-glass electromagnetic calorimeter. The correlation function is obtained after accounting for purity and resonant background. It is parametrised with a static picture of a Gaussian emitting source [1, 2].

2 Selection of hadronic Z^0 decays

A full description of the OPAL detector can be found in [13]. The sub-detectors relevant to the present analysis are the central tracking detector and the electromagnetic calorimeter. The central tracking detector consists of a silicon micro-vertex detector, close to the beam pipe, and three drift chamber devices: the vertex detector, a large jet chamber and surrounding z -chambers¹. In combination, the three drift chambers sitting inside a solenoidal magnetic field of 0.435 T yield a momentum resolution of $\sigma_{p_t}/p_t \approx \sqrt{0.02^2 + (0.0015 \cdot p_t)^2}$ for $|\cos(\theta)| < 0.7$, where p_t (in GeV) is the transverse momentum with respect to the beam axis. The electromagnetic calorimeter detects and measures the energies and positions of electrons, positrons and photons for energies above 0.1 GeV. It is a total absorbing calorimeter, and is mounted between the coil and the iron yoke of the magnet. It consists of 11704 lead-glass blocks arranged in three large assemblies (the barrel that surrounds the magnet coil, and two endcaps) which together cover 98% of the solid angle. The intrinsic energy resolution is $\sigma_E/E \simeq 5\%/\sqrt{E}$, where E is the electromagnetic energy in GeV.

Standard OPAL selection criteria are applied to tracks and electromagnetic clusters [14]. Tracks are required to have at least 20 measured points in the jet chamber, a measured momentum greater than 0.1 GeV, an impact parameter $|d_0|$ in the $r - \phi$ plane smaller than 2 cm, a z position at the point of closest approach to the origin in the $r - \phi$ plane within 25 cm of the interaction point, and a measured polar angle with respect to the beam axis greater than 20° . Electromagnetic clusters are required to have an energy greater than 0.1 GeV if they are in the barrel part of the detector (i.e. $|\cos\theta| \leq 0.82$) or greater than 0.3 GeV if they are in the endcap parts. Hadronic Z^0 decays are selected by requiring for each event

¹The OPAL coordinate system is defined so that the z axis is in the direction of the electron beam, the x axis points towards the centre of the LEP ring, and θ and ϕ are the polar and azimuthal angles, defined relative to the $+z$ - and $+x$ -axes, respectively. In cylindrical polar coordinates, the radial coordinate is denoted r .

more than 7 measured tracks, a visible energy larger than 60 GeV and an angle larger than 25° and smaller than 155° between the calculated event thrust [15] axis and the beam axis. The visible energy is the energy sum of all detected tracks, electromagnetic clusters not associated to tracks and electromagnetic clusters associated to tracks after correcting for double counting. A sample of 3.1 million Z^0 hadronic decays is selected for which the total background, consisting mainly of τ pairs, is less than 1% and is neglected throughout the analysis.

Detector effects and detection efficiencies for the spectra of π^0 pairs are evaluated using eight million Monte Carlo hadronic Z^0 decays. Events are generated using the JETSET 7.4 program, tuned to reproduce the global features of hadronic events as measured with the OPAL detector [14], with the BEC effect explicitly switched off. Samples generated with the HERWIG 5.9 program without the BEC effect are used for comparison. The generated events were passed through a full simulation of the OPAL detector [16] and were analysed using the same reconstruction and selection programs as were applied to the data.

3 Reconstruction of π^0 mesons

For the selected event sample, neutral pions are reconstructed from photon pairs. Photon reconstruction is performed in the barrel part of the electromagnetic calorimeter where both the photon reconstruction efficiency and the energy resolution are good. The procedure of [17] which resolves photon candidates in measured electromagnetic clusters is used. It employs a parametrisation of the expected lateral energy distribution of electromagnetic showers. It is optimised to resolve as many photon candidates as possible from the overlapping energy deposits in the electromagnetic calorimeter in a dense environment of hadronic jets. The purity of the photon candidate sample is further increased using a likelihood-type function [17] that associates to each photon candidate a weight w for being a true photon. Photon candidates with higher w are more likely to be true photons.

All possible pairs of photon candidates are then considered. Each pair was assigned a probability P for both candidates being correctly reconstructed as photons. This probability is simply the product of the w -weights associated with the two candidates. The combinatorial background consists of a mixture of three components: (i) wrong pairing of two correctly reconstructed photons, (ii) pairing of two fake photons and (iii) pairing of one correctly reconstructed photon with a fake one. Choosing only photon pairs with high values of P leaves combinatorial background mostly from component (i).

The π^0 reconstruction efficiency and purity are illustrated in Figure 1 for different cuts on P . The efficiency is defined as the ratio of the number of correctly reconstructed π^0 s over the number of generated π^0 s, and the π^0 purity is defined as the ratio of signal over total entries in a photon-pair mass window between 100 and 170 MeV.

OPAL

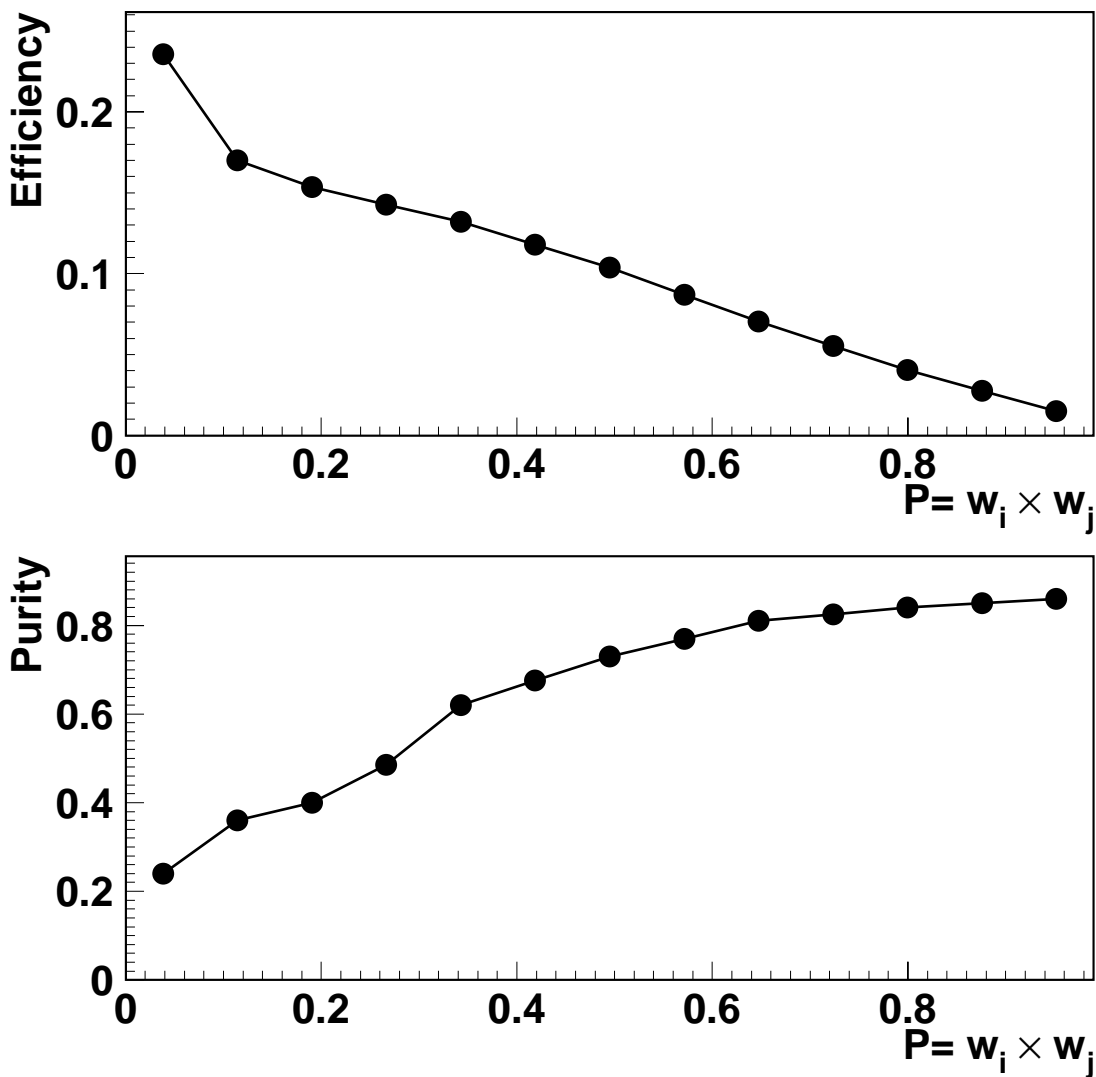


Figure 1: The π^0 reconstruction efficiency (top) and the purity (bottom) for different cuts on the weight $P = w_i \times w_j$ of the ij photon pair. The purity and efficiency are estimated from the JETSET Monte Carlo. The corresponding statistical errors are smaller than 1%.

4 Selection of π^0 Pairs

The average number of π^0 s produced in Z^0 decays has been measured [18] to be 9.76 ± 0.26 , which is reproduced by our Monte Carlo simulations. This leads to about 45 possible π^0 pairings per event. Considering only π^0 candidates with $P > 0.1$ (i.e. 17% efficiency and 36% purity), we reconstruct at the detector level 4.7 π^0 candidates on average per event. This leads to about 8 pairings among which only 1 pair on average is really formed by true π^0 s. Here, the detector level means that detector response, geometrical acceptance and photon reconstruction efficiency are taken into account. Therefore, the π^0 pair sample is background dominated and the study of π^0 pair correlations or invariant mass spectra is subject to very large background subtraction. Monte Carlo must be used to predict both the shape and amount of background to be subtracted, leading to large systematic errors in the measurements of the BEC source parameters.

To avoid this, the π^0 selection criteria are tightened. We select π^0 s which have a momentum above 1 GeV. This cut reduces the fraction of fake π^0 s. In addition, it removes π^0 s produced by hadronic interactions in the detector material for which the Monte Carlo simulation is not adequate. The probability P associated to each π^0 candidate is required to be greater than 0.6. In the case where a photon can be combined in more than one pair, only the pair with the highest probability is considered as a π^0 candidate. Among the events with four or more reconstructed photon candidates, only those leading to a possible π^0 pair with four distinct photon candidates are retained for further analysis. Events with six or more photon candidates leading to more than two π^0 candidates are rejected. They represent about 10% of the retained sample and would increase the sensitivity to unwanted resonance signals if they were not rejected. Figure 2 shows the photon pair mass, $M_{2\gamma}$, for the selected events. The average purity of the π^0 sample is 79% in the mass window between 100 and 170 MeV. The background is estimated directly from data by a second order polynomial fit to the side bands of the peak and by Monte Carlo simulation. The two background estimations yield compatible results and the Monte Carlo reproduces correctly the data. The superimposed curves are not the result of a fit to the data, but smoothed histograms of the Monte Carlo expectations for signal and background normalised to the total number of selected hadronic Z^0 decays.

A clear π^0 pair signal is obtained as shown in Figure 3 where the two values of $M_{2\gamma}$ are shown for the retained events. A π^0 pair is considered as a signal candidate if both values of $M_{2\gamma}$ are within the mass window between 100 and 170 MeV. The average π^0 pair signal purity is 60% and the Monte Carlo simulation describes the data well. Kinematic fits were made, constraining the mass of pairs of photon candidates to the π^0 mass, with the assumption that the photons come from the primary interaction vertex. Monte Carlo studies showed that this gives a 26% improvement in the resolution of the π^0 momentum.

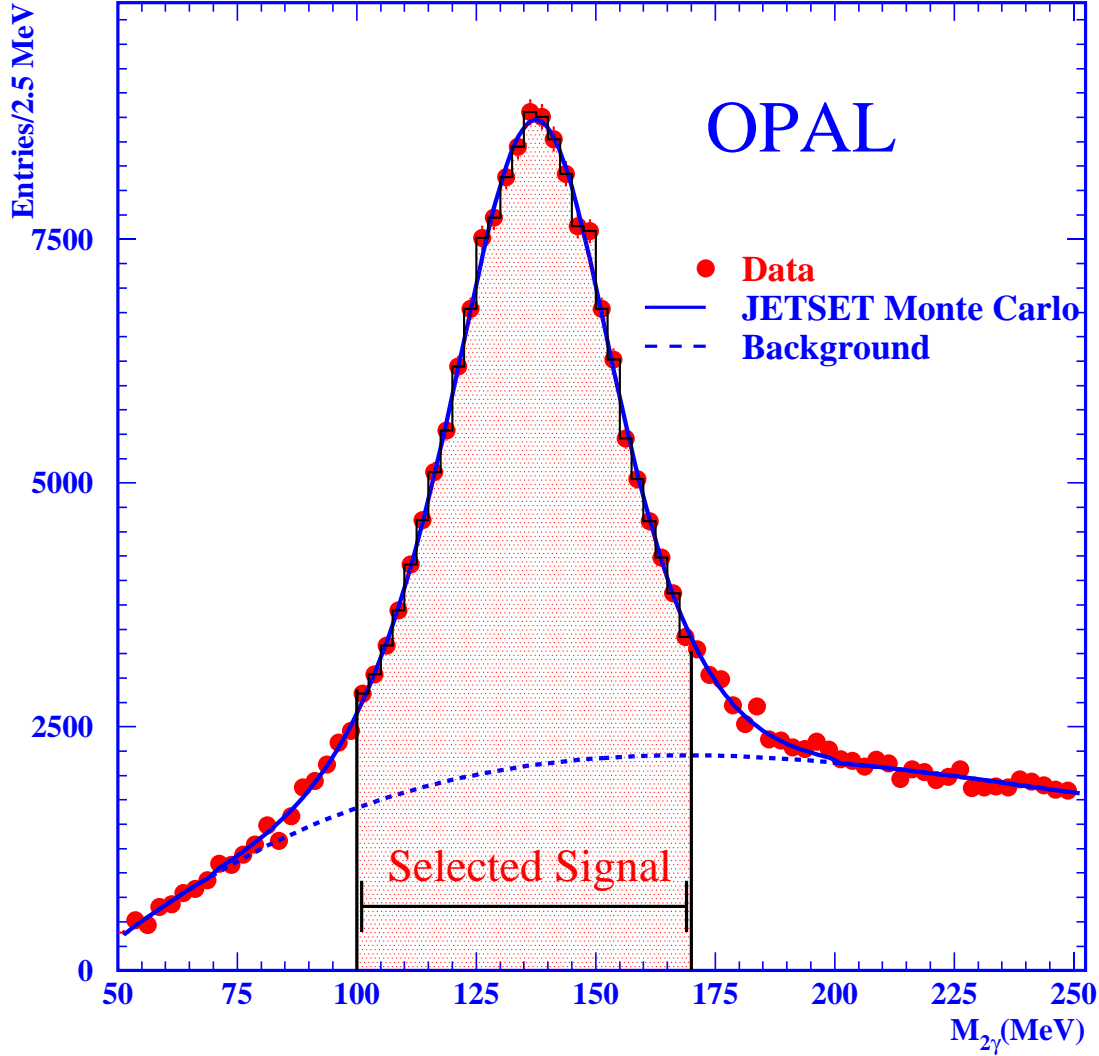


Figure 2: Distribution of two-photon invariant mass, $M_{2\gamma}$, for selected events which have exactly two reconstructed π^0 candidates per event. The smooth curves represent the total Monte Carlo expectation (solid line) and the background (dashed line) expectation. The curves are normalised to the same number of total selected hadronic Z^0 decays as in the data. The shaded region (100–170 MeV) represents the selected window for the π^0 signal.

OPAL

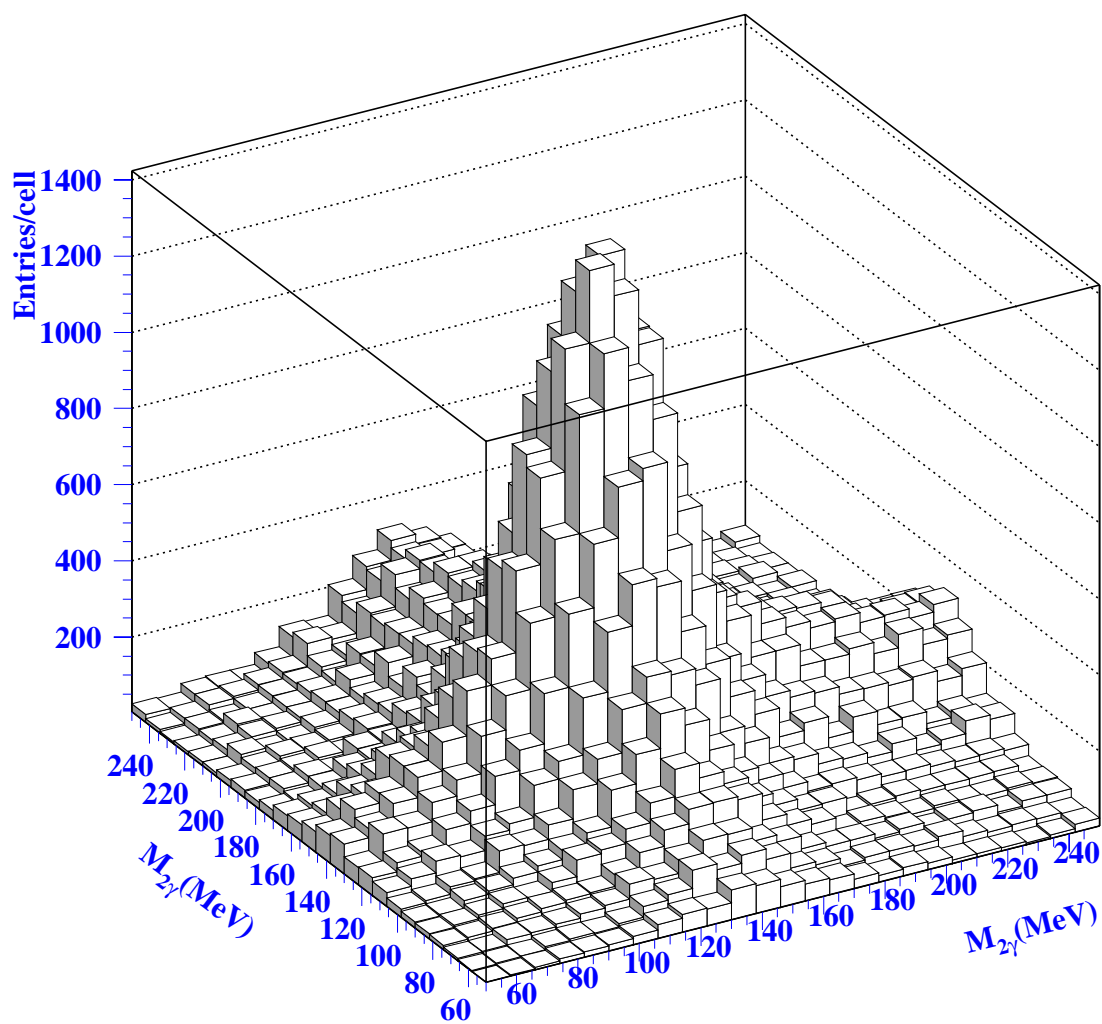


Figure 3: The two values of $M_{2\gamma}$ for each selected event. The cell size is $8 \times 8 \text{ MeV}^2$.

5 The BEC Function

The correlation function is defined as the ratio,

$$C(Q) = \frac{\rho(Q)}{\rho_0(Q)}, \quad (1)$$

where Q is a Lorentz-invariant variable expressed in terms of the two π^0 four-momenta p_1 and p_2 via $Q^2 = -(p_1 - p_2)^2$, $\rho(Q) = (1/N)dN/dQ$ is the measured Q distribution of the two π^0 s and $\rho_0(Q)$ is a reference distribution which should, in principle, contain all the correlations included in $\rho(Q)$ except the BEC. For the measurement of $\rho_0(Q)$, we consider the two commonly used methods [6]:

- **Event Mixing:** Mixed π^0 pairs are formed from π^0 s belonging to different Z^0 decay events in the data. To remove the ambiguity on how to mix events, we select two-jet events having a thrust value $T > 0.9$, i.e. well defined back-to-back two-jet events. The thrust axes of the two events are required to be in the same direction within $(\Delta \cos \theta \times \Delta \phi) = (0.05 \times 10^\circ)$. Mixing is then performed by swapping a π^0 from one event with a π^0 from another event. To avoid detection efficiency problems arising from different detector regions, swapping of two pions is performed only if they point to the same region of the electromagnetic barrel detector within $(\Delta \cos \theta \times \Delta \phi) = (0.05 \times 10^\circ)$. With this procedure, we start with two hadronic Z^0 events each having two π^0 candidates and can end up with between zero and four pairs of mixed π^0 candidates. The Q variable is then calculated for each of the mixed pairs. If the contributions from background are removed or suppressed, this method offers the advantage of being independent of Monte Carlo simulations, since $C(Q)$ can be obtained from data alone.
- **Monte Carlo Reference Sample:** The ρ_0 distribution is constructed from Monte Carlo simulation without BEC. The Monte Carlo is assumed to reproduce correctly all the other correlations present in the data, mainly those corresponding to energy-momentum conservation and those due to known hadron decays. In order to be consistent with the first method, the cut $T > 0.9$ is also applied for both data and Monte Carlo.

In the following, the distributions $\rho(Q)$ and $\rho_0(Q)$ are measured from the same sample of selected events. The mixing technique is used as the main analysis method and the Monte Carlo reference technique is applied only for comparison.

6 The Measured BEC Function and Background Contribution

The correlation function, $C(Q)$, corresponds experimentally to the average number of π^0 pairs, corrected for background, in the data sample divided by the corresponding cor-

rected average number in the reference sample. Thus, we can write

$$C(Q) = \frac{\rho(Q)}{\rho_0(Q)} = \frac{\rho^m(Q) - \rho^b(Q)}{\rho_0^m(Q) - \rho_0^b(Q)}, \quad (2)$$

where ρ^m and ρ_0^m are the measured values, and ρ^b and ρ_0^b are the corresponding corrections for background contributions. For both the numerator and denominator, the background consists mainly of π^0 pairs in which one or both π^0 candidates are fake.

The background distributions ρ^b and ρ_0^b are obtained from the Monte Carlo information. These background distributions can also be obtained from data using a side band fit to the projected spectra of the two-dimensional $M_{2\gamma}$ distributions (see Figure 3) in each 400 MeV interval of the measured Q variable. The resulting background distributions are correctly reproduced by Monte Carlo. However, for the smaller Q intervals as used in this analysis, i.e. 100 MeV, the side band fit is subject to large statistical fluctuations, so the Monte Carlo distributions have to be used.

In the region of interest where the BEC effect is observed, $Q < 700$ MeV, pion pairs from particle (resonance) decays could mimic the effect. The relevant decays are: $K_s^0 \rightarrow \pi^0\pi^0$, $f_0(980) \rightarrow \pi^0\pi^0$, and $\eta \rightarrow \pi^0\pi^0\pi^0$ with branching ratios of 39%, 33% and 32% respectively. Pion pairs from η decay contribute only to the region $Q < 315$ MeV. According to Monte Carlo studies, the number of reconstructed K_s^0 in the $2\pi^0$ channel is very small. Furthermore, the hypothesis that each π^0 originates from the primary vertex, as used in the kinematic fits (Section 4), does not apply. This is an advantage for this analysis since the K_s^0 peak is flattened, making its effect on the Q distribution negligible. The Monte Carlo estimates of this particle decay backgrounds are included in the distribution $\rho^b(Q)$, adjusting the rate of individual hadrons to the LEP average [18] where necessary.

For our analysis we select π^0 candidates with momentum greater than 1 GeV. This is dictated by the observation of correlations at small Q even for Monte Carlo events generated without any BEC effect. Indeed, as shown in Figure 4, a clear BEC-type effect is visible in the correlation function obtained from Monte Carlo events without BEC for different low cuts on π^0 momentum. Using Monte Carlo information, we find that these correlations are mainly caused by π^0 s originating from secondary interactions with the detector material. They would constitute an irreducible background to the BEC effect if low momentum π^0 s are considered in the analysis. This effect vanishes for π^0 momenta greater than 1 GeV.

We rely on Monte Carlo simulation only to define the appropriate momentum cut (i.e. 1 GeV) which completely suppresses the effect of soft pions produced in the detector material, rather than relying on its prediction for the exact shape and size of this effect. The reason is that, in contrast to charged pions where the measured track information can be used to suppress products of secondary interactions in the detector material, the neutral pions have to be assumed to originate from the main interaction vertex. Furthermore, with this assumption the kinematic fits (Section 4) bias the energy of soft pions emitted in the detector material towards larger values since the real opening angle between the photons is larger (vertex closer to the calorimeter) than the assumed one.

With the above selection criteria, the composition of the selected π^0 pair sample is

studied using Monte Carlo simulations. According to the string fragmentation model implemented in JETSET, the selected sample consists of about 97.9% of mixed pion-pairs from different hadron decays, 2% of pairs belonging to the decay products of the same hadron and only 0.1% prompt pairs from the string break-ups. Similarly, using the cluster fragmentation model implemented in HERWIG, the selected sample consists of 97% of pairs from different hadron decays, 2.3% belonging to the decay products of the same hadron and only 0.7% originating directly from cluster decays. It is worth mentioning that even if the direct pion pairs from string break-up (JETSET) or cluster decays (HERWIG) were all detected and accepted by the analysis procedure, they would be diluted in combination with other pions and would constitute only a marginal fraction ($< 1\%$) of the total number of reconstructed π^0 pairs. Thus, our analysis has no sensitivity to direct pion pairs originating from string break-up or cluster decay.

7 Results

The correlation distribution $C(Q)$ (Eq. (2)) is parametrised using the Fourier transform of the expression for a static sphere of emitters with a Gaussian density (see e.g. [19]):

$$C(Q) = N(1 + \lambda \exp(-R^2 Q^2))(1 + \delta Q + \epsilon Q^2). \quad (3)$$

Here λ is the chaoticity of the correlation [which equals zero for a fully coherent (non-chaotic) source and one for a chaotic source], R is the radius of the source, and N a normalisation factor. The empirical term, $(1 + \delta Q + \epsilon Q^2)$, accounts for the behaviour of the correlation function at high Q due to any remaining long-range correlations. The $C(Q)$ distribution for data is shown in Figure 5 as the points with corresponding statistical errors, and the smooth curve is the fitted correlation function in the Q range between 0 and 2.5 GeV. A clear BEC enhancement is observed in the low Q region of the distribution. The parameters are determined to be:

$$\begin{aligned} \lambda &= 0.55 \pm 0.10, \\ R &= (0.59 \pm 0.08) \text{ fm}, \\ N &= 1.10 \pm 0.08, \\ \delta &= (-0.14 \pm 0.05) \text{ GeV}^{-1}, \\ \epsilon &= (0.07 \pm 0.03) \text{ GeV}^{-2}, \end{aligned}$$

where the quoted errors are statistical only and the χ^2/ndf of the fit is 14.7/19.

The distribution $C(Q)$ obtained for Monte Carlo events generated with no BEC is shown as a histogram in the same figure. It shows that there is no residual correlation at low Q and indicates that the observed enhancement is present in the data only. The dashed-line histogram of Figure 5 represents the correlation function obtained from data but before the subtraction, using the Monte Carlo estimates, of pairs from the decay products of the same hadron, indicating that these contributions have only a minor influence on the measured parameters. In addition, the correlation function constructed with background π^0 pairs does not show any enhancement at low Q (not shown). Here, background π^0 pairs are defined as pairs for which one or both of the π^0 s are outside the mass window 100-170 MeV, i.e. these are likely to be fake π^0 candidates.

Monte Carlo without BEC

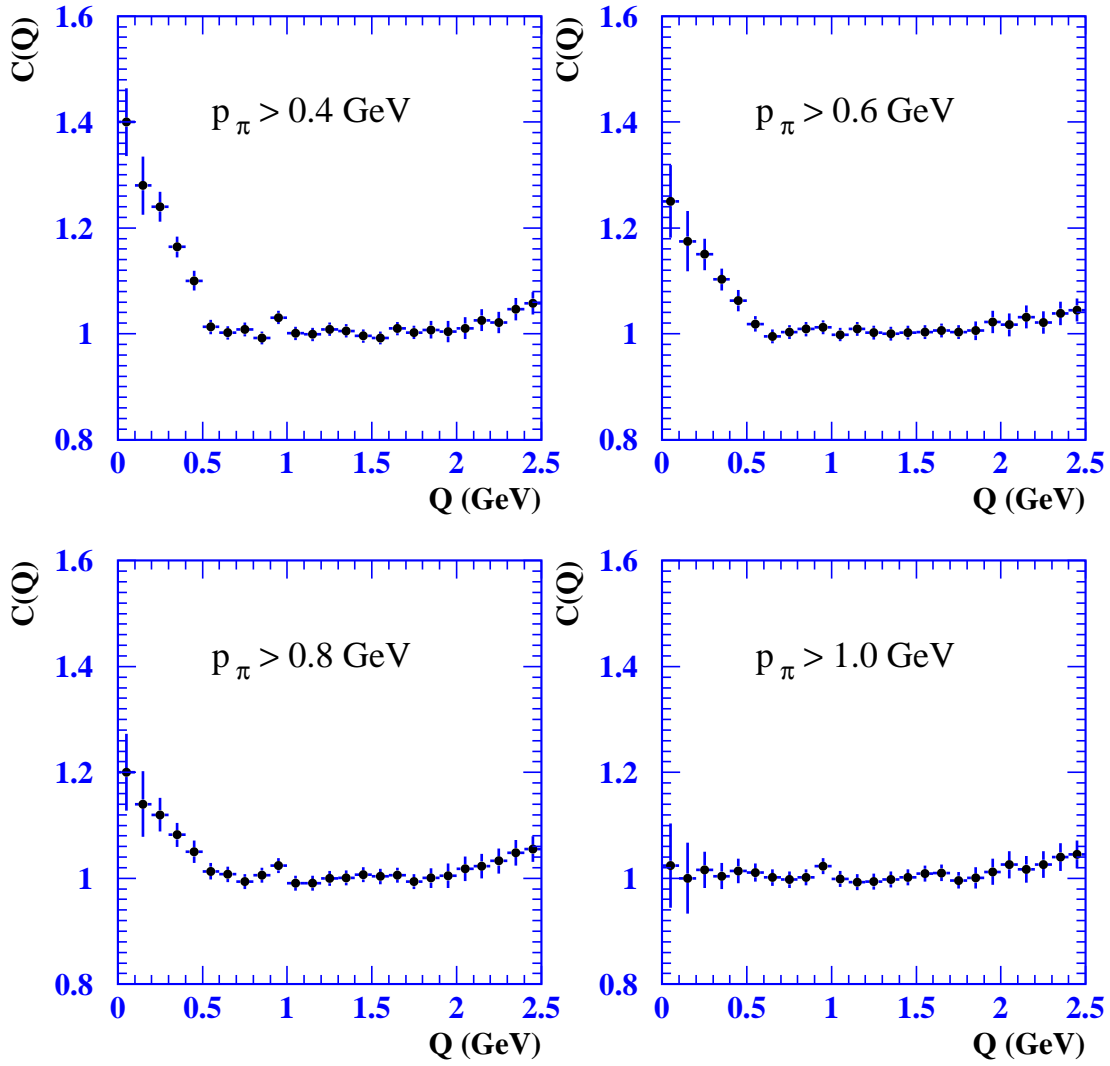


Figure 4: The correlation distribution $C(Q)$ determined for JETSET Monte Carlo events (generated without BEC effect) for different cuts on the π^0 momenta, p_π .

The second method, which uses the MC reference sample, yields the following results:

$$\begin{aligned}\lambda &= 0.50 \pm 0.10, \\ R &= (0.46 \pm 0.08)\text{fm}.\end{aligned}$$

These results are quoted for comparison only. We choose to quote the results obtained with the event mixing method since they are much less dependent on details of the Monte Carlo modelling.

The string model predicts a smaller source radius and a larger chaoticity in the BEC effect for π^0 pairs than for π^\pm pairs, while the cluster model predicts no difference. These predictions hold only for prompt boson pairs produced directly from the string or cluster decays. According to our Monte Carlo simulations, we have no sensitivity to these pairs.

8 Systematic Uncertainties

Potential sources of systematic error are investigated. In each case the effect on the parameters R and λ and their deviations with respect to the standard analysis are estimated. The results are summarised in Table 1.

- **Bin width resolution:** After the kinematic fits (Section 4), the resolution on the invariant mass of two pions, or on the variable Q , is approximately 60 MeV. We have chosen a bin width of 100 MeV for the fit to the measured $C(Q)$ distribution. This bin width is varied from 100 MeV to 80 MeV and to 120 MeV.
- **Fit range:** The low end of the fit range is set to start at $Q = 350$ MeV (fourth bin) The high end of the fit range is changed to stop at $Q = 2$ GeV.
- **Effect of hadron decays:** To estimate the effect of the π^0 pairs from the same resonance decay on the measured BEC parameters, the estimated contribution is varied by $\pm 10\%$ which represents the typical error on the measured individual hadron rates [18]. In order to investigate the dependence of the measured parameters R and λ on the π^0 momentum cut, the analysis is repeated for π^0 momenta larger than 1.2 GeV.
- **Analysis procedure:** The analysis is repeated for several variations of the selection criteria.
 - **1)** The π^0 selection mass window is changed from 100-170 MeV to 110-165 MeV (increases the π^0 purity by 5%).
 - **2)** The probability for π^0 selection is changed from 0.6 to 0.5 (reduces the π^0 purity by 5%).
 - **3)** The thrust value for two-jet events is changed from 0.9 to 0.85 and to 0.92 (changes the overall event sample size by $\pm 5\%$).
 - **4)** The factor $1 + \delta Q + \epsilon Q^2$ is replaced by $1 + \delta Q$.

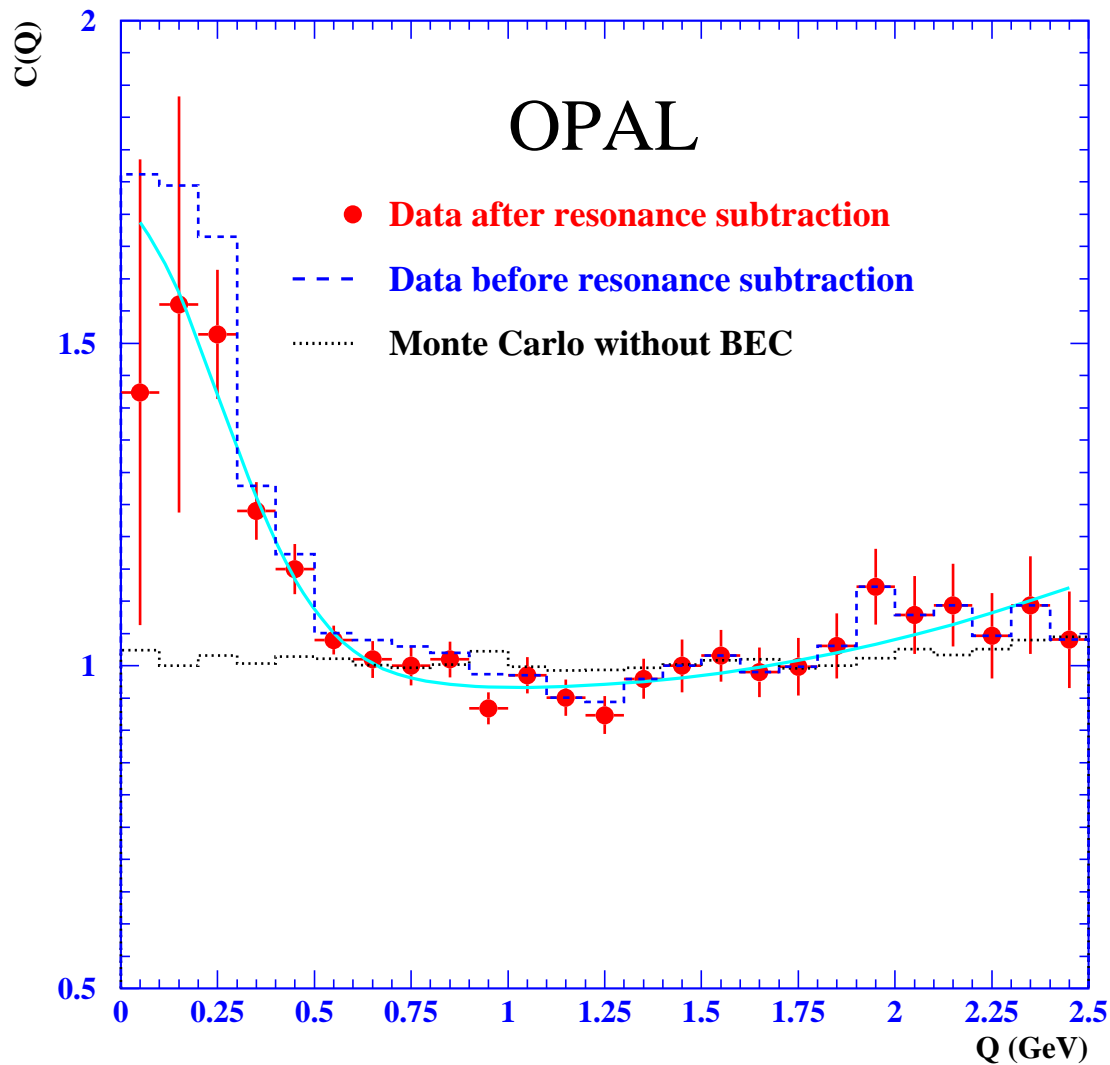


Figure 5: The correlation distribution $C(Q)$ as measured for OPAL data. The smooth curve is the fitted correlation function and the dotted histogram is the correlation distribution obtained for JETSET Monte Carlo events generated without BEC. The dashed histogram represents the measured correlation function before the subtraction of the contributions from known hadron decays.

- 5) π^0 from different events are mixed if they point to the same region of the detector within $(\Delta \cos \theta \times \Delta \phi) = (0.10 \times 15^\circ)$ instead of $(0.05 \times 10^\circ)$.

The final systematic errors are obtained from quadratically adding the deviations from the central value. Thus,

$$\begin{aligned}\lambda &= 0.55 \pm 0.10 \pm 0.10, \\ R &= (0.59 \pm 0.08 \pm 0.05) \text{ fm}.\end{aligned}$$

9 Conclusions

We have observed Bose-Einstein correlations of π^0 pairs produced in hadronic Z^0 decays. Assuming a Gaussian shape for the source, we obtain $\lambda = 0.55 \pm 0.10 \pm 0.10$ for the chaoticity parameter and $R = (0.59 \pm 0.08 \pm 0.05)$ fm for the radius. In order to construct a reference sample with the event mixing method, this analysis is restricted to well defined back-to-back two-jet events. Furthermore, in order to remove π^0 s not originating from the primary interaction vertex the considered momentum phase space is restricted to $p_{\pi^0} > 1$ GeV. The measured value of the source radius is smaller than our former value [20], $R = (1.002 \pm 0.016_{-0.096}^{+0.023})$ fm, obtained for charged pions for which the measured track parameters allowed access to lower momenta and where the reference sample was constructed with unlike-sign pion pairs. However, the value is compatible with the LEP inclusive average [21], $R = (0.74 \pm 0.01 \pm 0.14)$ fm, for charged pions. Pions from strong decays constitute the dominant part of our sample of reconstructed π^0 pairs. We have no sensitivity to test the string or cluster model predictions concerning differences between neutral and charged pion pairs. We deduce that Bose-Einstein correlations exist between π^0 pairs in which each π^0 is a strong decay product of a different hadron.

Acknowledgements

We particularly wish to thank the SL Division for the efficient operation of the LEP accelerator at all energies and for their close cooperation with our experimental group. In addition to the support staff at our own institutions we are pleased to acknowledge the Department of Energy, USA, National Science Foundation, USA, Particle Physics and Astronomy Research Council, UK, Natural Sciences and Engineering Research Council, Canada, Israel Science Foundation, administered by the Israel Academy of Science and Humanities, Benozio Center for High Energy Physics, Japanese Ministry of Education, Culture, Sports, Science and Technology (MEXT) and a grant under the MEXT International Science Research Program, Japanese Society for the Promotion of Science (JSPS),

Table 1: Systematic errors

| <i>Item</i> | λ | R [fm] | $\Delta\lambda$ | ΔR |
|------------------------------------|-----------------|-----------------|-----------------|------------|
| Basic result | 0.55 ± 0.10 | 0.59 ± 0.08 | +0.00 | +0.00 |
| Bin width=80 MeV | 0.54 ± 0.13 | 0.58 ± 0.12 | -0.01 | -0.01 |
| Bin width=120 MeV | 0.57 ± 0.09 | 0.60 ± 0.07 | +0.02 | +0.01 |
| Low end of the Fit range = 350 MeV | 0.64 ± 0.14 | 0.62 ± 0.12 | +0.09 | +0.03 |
| High end of the Fit range = 2 GeV | 0.58 ± 0.11 | 0.56 ± 0.10 | +0.03 | -0.03 |
| Resonance contribution +10% | 0.54 ± 0.10 | 0.59 ± 0.08 | -0.01 | +0.00 |
| Resonance contribution -10% | 0.55 ± 0.10 | 0.58 ± 0.09 | -0.00 | -0.01 |
| Momentum cut = 1.2 GeV | 0.53 ± 0.11 | 0.60 ± 0.08 | -0.02 | +0.01 |
| Analysis procedure: | | | | |
| 1) π^0 -signal mass window | 0.55 ± 0.10 | 0.58 ± 0.09 | +0.00 | -0.01 |
| 2) Photon-pair probability | 0.57 ± 0.09 | 0.57 ± 0.08 | +0.02 | -0.02 |
| 3) Thrust value | 0.55 ± 0.10 | 0.60 ± 0.09 | +0.00 | +0.01 |
| 4) Long range corr. term | 0.56 ± 0.10 | 0.58 ± 0.10 | +0.01 | -0.01 |
| 5) Mixing condition | 0.54 ± 0.08 | 0.59 ± 0.07 | -0.01 | +0.00 |
| Total sys. error | | | 0.10 | 0.05 |

German Israeli Bi-national Science Foundation (GIF),
 Bundesministerium für Bildung und Forschung, Germany,
 National Research Council of Canada,
 Hungarian Foundation for Scientific Research, OTKA T-029328, and T-038240,
 The NWO/NATO Fund for Scientific Research, the Netherlands.

References

- [1] G. Goldhaber, S. Goldhaber, W. Lee and A. Pais, Phys. Rev. 120 (1960) 130.
- [2] R. Hanbury Brown and R.Q. Twiss, Phil. Mag. 54 (1954) 633;
 R. Hanbury Brown and R.Q. Twiss, Nature 178 (1956) 1046.
- [3] L. Lönnblad and T. Sjöstrand, Phys. Lett. B351 (1995) 293;
 V.A. Khoze and T. Sjöstrand, Eur. Phys. J. C6 (1999) 271.
- [4] T. Sjöstrand and M. Bengtsson, Comp. Phys. Comm. 43 (1987) 367.
- [5] G. Marchesini and B.R. Webber, Nucl. Phys. B310 (1988) 461;
 G. Marchesini *et al.*, Comp. Phys. Comm. 67 (1992) 465.
- [6] For recent reviews see:
 K. Zalewski, Lectures at 40th Course of Cracow School of Theoretical Physics, Zakopane (Poland), 2000, Acta Phys. Polonica B31 (2000) 2819;
 W. Kittel, Lectures at 41st Course of Cracow School of Theoretical Physics, Zakopane (Poland), 2001, Acta Phys. Polonica, B32 (2001) 3927;

- R. M. Weiner, Phys. Rep. 327 (2000) 249;
U. A. Wiedemann and U. Heinz, Phys. Rep. 319 (1999) 145.
- [7] L3 Collaboration, P. Achard *et al.*, Phys. Lett. B524 (2002) 55;
K. Eskreys, Acta Phys. Pol. 36 (1969) 237;
V.G. Grishin *et al.*, Sov. J. Nucl. Phys. 47 (1988) 278;
O. Kortner *et al.*, Eur. Phys. J. C25 (2002) 353.
- [8] B. Andersson and M. Ringnér, Nucl. Phys. B513 (1998) 627.
- [9] K. Zalewski, Nucl. Phys. (Proc. Suppl.) B96 (2001) 23.
- [10] B. Andersson and W. Hofmann, Phys. Lett. B169 (1986) 364.
- [11] I. A. Andreev *et al.*, Phys. Rev. Lett. 67 (1991) 3478.
- [12] M.G. Bowler, Phys. Lett. B197 (1987) 443;
M. Suzuki, Phys. Rev. D35 (1987) 3359;
M. Biyajima *et al.*, Phys. Rev. C58 (1998) 2316;
G. Alexander and H.J. Lipkin, Phys. Lett. B456 (1999) 270.
- [13] OPAL Collaboration, K. Ahmet *et al.*, Nucl. Instr. and Meth. A305 (1991) 275;
OPAL Collaboration, P.P. Allport *et al.*, Nucl. Instr. and Meth. A324 (1993) 34;
OPAL Collaboration, P.P. Allport *et al.*, Nucl. Instr. and Meth. A346 (1994) 476.
- [14] OPAL Collaboration, G. Alexander *et al.*, Z. Phys. C69 (1996) 543;
OPAL Collaboration, K. Ackerstaff *et al.*, Phys. Lett. B388 (1996) 659.
- [15] T. Sjöstrand, Comp. Phys. Comm. 82 (1994) 74.
- [16] OPAL Collaboration, J. Allison *et al.*, Nucl. Instr. and Meth. A317 (1992) 47.
- [17] OPAL Collaboration, G. Abbiendi *et al.*, Eur. Phys. J. C17(2000) 373.
- [18] The Review of Particle Physics, PDG, K. Hagiwara *et al.*, Phys. Rev. D66 (2002) 010001-256.
- [19] OPAL Collaboration, G. Abbiendi *et al.*, Eur. Phys J. C21 (2001) 23.
- [20] OPAL Collaboration, G. Abbiendi *et al.*, Eur. Phys. J. C16 (2000) 423.
- [21] G. Alexander, I. Cohen and E. Levin, Phys. Lett. B452 (1999) 159.